IEEE Access
Multidisciplinary | Rapid Review | Open Access Journal

Received April 6, 2021, accepted April 26, 2021, date of publication May 17, 2021, date of current version June 2, 2021.

Digital Object Identifier 10.1109/ACCESS.2021.3080687

Different Eye Movement Behaviors Related to Artificial Visual Field Defects–A Pilot Study of Video-Based Perimetry

CHANGTONG MAO[1,2], KENTARO GO[2], (Member, IEEE), YUICHIRO KINOSHITA[2], (Member, IEEE), KENJI KASHIWAGI[3], MASAHIRO TOYOURA[2], (Member, IEEE), ISSEI FUJISHIRO[4], (Senior Member, IEEE), JIANJUN LI[1], AND XIAOYANG MAO[2], (Member, IEEE)

[1]College of Computer Science and Technology, Hangzhou Dianzi University, Hangzhou 310018, China
[2]Department of Computer Science and Engineering, University of Yamanashi, Kofu 400-8511, Japan
[3]Department of Ophthalmology, University of Yamanashi, Chuo 409-3898, Japan
[4]Center for Information and Computer Science, Keio University, Yokohama 223-8522, Japan

Corresponding authors: Kentaro Go (go@yamanashi.ac.jp) and Changtong Mao (g18tka18@yamanashi.ac.jp)

This work was supported by the JSPS KAKENHI under Grant 17H00738, Grant 19H05472, and Grant 19H05576.

This work involved human subjects or animals in its research. Approval of all ethical and experimental procedures and protocols was granted by the IRB.

ABSTRACT Visual field defects (VFDs) can be caused by numerous diseases, some of which (e.g., glaucoma) are the main causes of blindness in humans. The present perimetry, which is defined as the measurement of visual field function, has high requirements for patients such as long-term fixation and reliable interaction with the system. In this pilot study, we combined the videos and eye-tracking techniques in a free-watching task and explored the different eye movement behaviors of people with several types of artificial VFDs, such as hemianopia, altitudinal VFDs, and tunnel vision. We carried out the task in a gaze-contingent modality where 38 participants with normal vision were recruited to watch a group of videos monocularly. The eye gaze data were recorded by the tracker during the task. We hypothesized that people with simulated VFDs will produce a more active eye movement coping mechanism to compensate for their visual field disadvantage. A new measurement called eye movement amount (MA) was proposed to describe the amount of eye movement toward a specific direction. Statistically significant differences caused by artificial VFDs were observed by comparing the MA values between the VFD groups and the control group. In addition, we found artificial hemianopia and inferior VFDs lead participants to produced increased MA in the horizontal and vertical directions respectively. Artificial tunnel vision, on the contrary, induces a decreased MAs in both horizontal and vertical directions. The proposed metrics can be used as potential biomarkers for distinguishing VFDs in a free-watching task.

INDEX TERMS Gaze tracking, visual field defect, perimetry, eye biomarkers.

I. INTRODUCTION

Visual field defect (VFD) is defined as a loss of part of the usual visual field. It can be caused by numerous conditions, including glaucoma, macular degeneration, and brain tumors, which are also considered the leading cause of blindness in humans [1]. In most cases, VFDs can be irreversible and even progressive and directly affect people's quality of life [2]. Thus, early detection of VFDs is crucial for diagnosing the underlying causes and monitoring the gradual progression of eye conditions [3].

There are numerous techniques for visual field assessment and they can be categorized into two branches, including kinetic and static perimetry. In kinetic perimetry, the

The associate editor coordinating the review of this manuscript and approving it for publication was Donato Impedovo.

Goldmann kinetic perimetry defines an isopter by moving the stimulus with set size and intensity from the non-seeing area to the seeing area, along with a set of equidistant meridians. Then, it constructs a vision island by these isopters. This method has been used often in young children [4], [5]. In static perimetry, standard automated perimetry (SAP), which uses static stimuli (i.e., constant size and location) to measure the threshold sensitivity of specific retina locations, provides a comprehensive statistical analysis of the results and has become the gold standard for visual field assessment. However, inevitable challenges exist when it comes to the test. First, even if the algorithm proposed previously can substantially reduce the test duration (e.g., SITA [6]–[8]), both perimetries still require patients to maintain fixation for a prolonged period. This may cause the participants to feel tired and uninterested. Second, these assessments are typically performed using dedicated devices (e.g., Humphrey visual field analyzer [HFA]), thus making home monitoring impossible. Moreover, it is also inconvenient for patients living in remote areas as the presence of experienced examiners is required for necessary guidance. Third, all participants must wait for the appearance of the stimuli and react by holding a buzzer. This design uses motor response as a proxy for the human visual perception, which increases the response variability, and a requirement of good cognitive function limits its uses in some age groups(e.g., the elderly and children). In fact, many patients find the application of SAP difficult [9].

To liberate the eyes of the participants and lower the difficulty of the test, we used a combination of eye-tracking techniques and a video-based task to explore the correlation between the eye movement patterns and the VFDs. Moreover, we simulated five types of VFDs, including hemianopia, altitudinal VFDs, and tunnel vision in people with normal vision. Through this simulation, we were able to collect data from a cohort group in a short time, and the variability (e.g., scotoma shape, participants' ages) among subjects has been controlled. We used an eye tracker to collect gaze data from participants by recording their eye movements when watching videos. By analyzing the participants' gaze movements, we found that when people with artificial scotoma watch videos, their eye movements patterns are significantly different from those of people with normal vision. Furthermore, the movement patterns were found to be associated with artificial VFDs, suggesting that video watching is a promising test format to detect visual field loss.

The contributions of this research are two-fold. First, we further explored a novel test modality, in which participants are asked to watch videos and the gaze data are recorded by an eye tracker. This approach effectively overcomes the drawbacks of SAP. Second, we explored the different eye behavior patterns by comparing the proposed metrics, which can be used as potential biomarkers of eye conditions. This work is an extended version of our previous study [10], which also explored the different gaze movement patterns with the presence of artificial VFDs. We tested more VFD types and recruited more participants accordingly.

II. RELATED WORK

A. IMPORVEMENT TO CONVENTIONAL PERIMETRY

In general, the demanding requirement of gaze, dedicated test device, and interaction modality are the main shortcomings of conventional perimetry. Several studies have obviated these with the help of an eye tracker, which has become an accessible technique in recent years [11]. Suprathreshold saccadic vector optokinetic perimetry (SVOP) [12], [13], which only uses a tracker and a personal computer, was originally developed for kids who have problems in undergoing the conventional perimetries [14]–[17]. Such a technique has also been made available to adults [18]. SVOP participants are asked to maintain fixation on the presented stimuli. Then, the system determines whether the participants were able to perceive the stimuli based on the amplitude and direction of the gaze movements. The threshold version of SVOP [19], [20] employs a threshold testing strategy that requires a considerable amount of time to achieve a more comprehensive evaluation. Jones *et al.* [21] proposed Eyecatcher, which only uses a tablet computer and an affordable clip-on eye tracker. This design significantly improved the portability of the test. In addition, they proposed the "Mean Hit Rate," which is comparable to the HFA's MD metric and can be used as a potential metric for assessing eye conditions. They recently released Eyecatcher V2 [22], in which the applicability of rapid triage in a real clinical scenario is tested. The result indicated a promising future for clinical triage. These research studies are essentially an extension of SAP, i.e., they reflect the sensitivity of predetermined locations on the retina by chasing explicit stimuli.

B. EYE MOVEMENT AND VISUAL FIELD DEFECTS

Previous studies have explored the links between eye movement and VFDs in multiple circumstances. Cornelissen *et al.* [23] and Bertera and Rayner [24] simulated central loss and tunnel vision with a varied scotomas size and investigated the adaptation of fixation durations to artificial VFDs in a target-searching task. The result indicates that simulated VFDs limit the visual system's ability and increase the difficulty of foveal analysis. Similarly, Smith *et al.* [25] confirmed that VFDs caused by glaucoma drive patients to require more time to search for a target. In detail, when patients perform searching or engaged in a free-viewing task related to everyday scenes, a significant reduction in the number of saccades was found [26], [27]. In addition, Asfaw *et al.* [28] compared eye-movements parameters between the worse eye and the better eye in glaucoma patients and found that the eye with VFDs will produce more "reversal" saccades. Chen *et al.* [29] reported that people with simulated VFDs need a greater saccade reaction time compared to the normal control. Cajar *et al.* [30], [31] explored the effects of the spatial frequency of artificial VFDs on eye movements in a scene-viewing task, showing that saccade amplitudes increase with central loss and decrease with tunnel vision. Geringswald *et al.* [32] demonstrated that

impairment of foveal vision leads to an increased fixation duration and inhibited saccade. Crabb *et al.* [33] performed a hazard perception test on glaucoma patients and proved that patients compensate for their restricted visual field by increasing the number of saccades and fixation while decreasing the fixation duration. In [34], the authors used a virtual driving simulator to evaluate the driving performance of glaucoma patients in hazardous situations. Showing patients coped with the same mechanism (i.e., increased number of saccades and decreased fixation duration).

C. ATTEMPTING OF NEW ASSESSMENT METHOD

A few studies explore the possibility of inferring VFDs from gaze data by watching videos or images. David *et al.* [35] extracted multiple features of gaze data from a free-viewing task and tried to find the best set to differentiate between artificial VFDs. Hidden Markov models and recurrent neural networks were used respectively to build the classifier. Similarly, Crabb *et al.* [36] recorded the eye movements of glaucoma patients while watching videos. A set of features was extracted by kernel principal component analysis on a saccade map, and these features were used as the input of a Naïve Bayes classifier that separated the patients from the controls. Asfaw *et al.* [37] simulated artificial VFDs from a real glaucoma patient and performed a free-viewing task using both images and videos. They evaluated the clinical usefulness of four eye-movement parameters by plotting receiver operating characteristics curves. Gestefeld *et al.* [38] simulated five common VFDs in a video-watching task and trained a linear support vector machine using the input of a fixation map, and this classifier was used to identify the presence of artificial VFDs. Furthermore, they reconstructed the VFDs, which can be a reference for visual field situations. In this study, we also used video as a task stimulus, and we considered a video with a changing frame to be more informative than other stimuli (e.g., bright light, images). In detail, for the people with normal vision, every change in the videos is exposed to the whole visual field, whereas people with VFDs inevitably miss parts of them, so this gap may trigger a more active gaze movement coping mechanism.

III. METHODS

A. EXPERIMENT OVERVIEW

We developed a gaze-contingent video-watching task by combining an eye tracker and various types of video clips. The tracker returns the gaze data of the participants when watching videos, and these data are used to simulate the VFD in "real-time." A group of students with a healthy visual field was recruited to watch videos monocularly through the simulation system. A small group of these participants watched additional videos for the test-retest repeatability analysis. Some of the participants were asked to simulate one type of VFD (i.e., hemianopia, altitudinal VFD, and peripheral loss).

B. PARTICIPANTS

The participants were 38 university students (age range: 21–37 years, mean age: 24.1 ± 2.9 years, 26 males and 12 females.) They all reported normal or correct-to-normal vision, and none had a history of macular degeneration, glaucoma, or other neurological disorders that may cause visual field loss. Except for one participant who reported a previous experience with eye-tracking devices and visual field assessment, the remaining participants were completely blinded to the experiment and never used an eye tracker or previously watched the video clips. One participant was excluded from the experiment due to the inability of the tracker to continuously record the gaze information, even after multiple attempts. The remaining 37 participants completed the experiment and our analyses were based on these individuals. The informed consent form was signed before the test, and the participants were compensated afterward. Our research plan was reviewed and approved by the Interdisciplinary Graduate School IRB, University of Yamanashi.

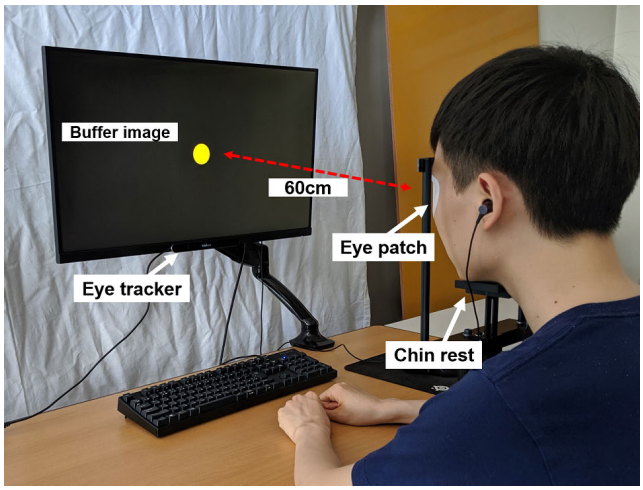

FIGURE 1. Experiment apparatus. The participants sat 60 cm away from the display (stabilized by a chin rest) and underwent the test monocularly. The eye tracker was mounted at the bottom of the display and automatically recorded eye movements during the trials. The test started with a buffered image to anchor the participants' fixation.

C. APPARATUS

Figure 1 describes the experiment apparatus. The stimuli were displayed on a 27″ LCD monitor (VL278, ASUS, Taiwan) with a 60 Hz refresh rate, and 1920 × 1080 pixels. The viewing distance was set to 60 cm, and the visual angle was 52.8° × 31.3° when fixated at the screen's center. Information on eye gaze was recorded by the Tobii Nano eye tracker (Tobii Technology, Sweden) at a sampling rate of 60 Hz, with a spatial accuracy of ≤0.3°. The tracker was attached to the bottom of the screen. This whole combination was integrated using an adjustable stand as the participants did not have the same height. In this test, a chin rest was also applied to prevent the participants from making significant head displacements and to enable them to focus on the video

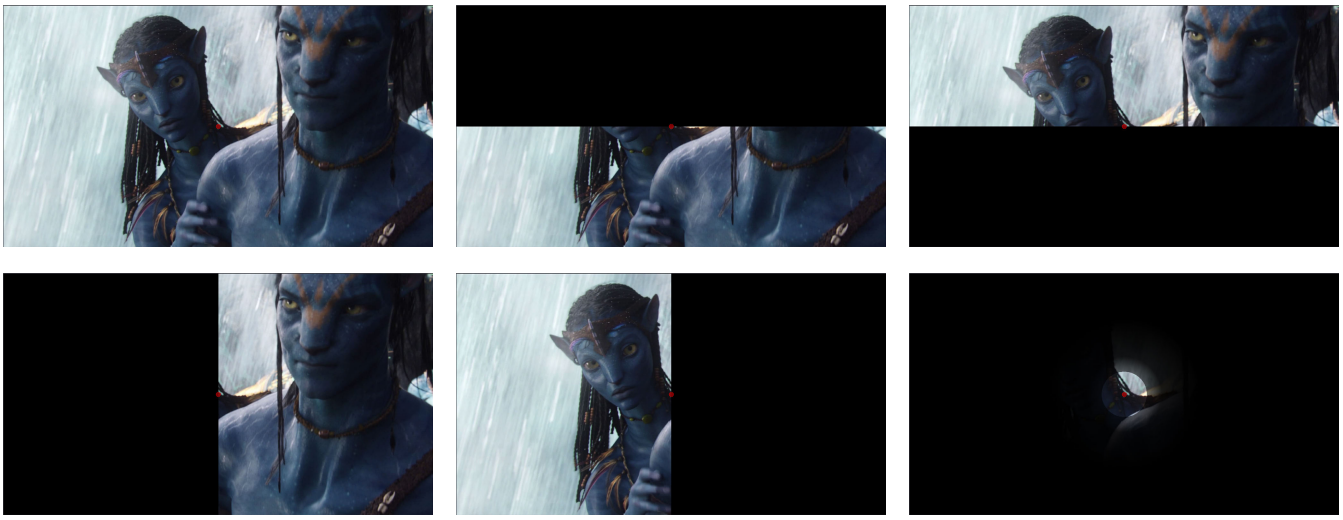

FIGURE 2. Presentation of six eye conditions–the top row from left to right represents the normal pattern, superior VFD, and inferior VFD. The bottom row from left to right represents left hemianopia, right hemianopia, and tunnel vision. Note that the simulated visual field loss was moved along with the participants' gaze. The figures represent the displayed content when the participants fixate at the center red anchor dot. (The sample image was captured from the SAVAM dataset.[1])

content. The participants wore an eye patch on their non-dominant eye.

Compared with SAP, this setup is more user-friendly and significantly reduces the participant requirements. Moreover, it is more affordable and portable. This modality provides the possibility for home monitoring.

D. STIMULI AND GAZE-CONTINGENT SIMULATION

In this research, a video dataset, called SAVAM [39], was selected to replace the traditional white-on-white stimulus. SAVAM consists of 41 videos, which can be divided into movie clips, sports video clips, and homemade videos. The content of the videos varies. Some videos show several objects on a simple background (e.g., sea, trees) without much scene change, while others show several objects and much information in a short period in a complex environment. All videos have the same properties, such as a fixed 25 fps frame rate, 1920 × 1080 resolution, and no audio channel. A 3-s buffer image (Figure 1) was stacked at the beginning of each video, as we wanted every participant to have the same start gaze location before the actual video. The test video was a combination of a few videos, and the duration was set to less than 2 minutes. Moreover, two *Tom & Jerry* animation clips (Ep63 ''Flying Cat'' and Ep46 ''Tennis Chumps'') were used for the experiment's repeatability analysis. These videos have the same properties as the SAVAM videos, with durations of 250 and 173 s, respectively.

We simulated five types of VFDs (Figure 2), including hemianopia (left and right), altitudinal VFDs (superior and inferior), and peripheral loss (i.e., tunnel vision). All the conditions were absolute scotoma. Hemianopia and altitudinal VFDs were simulated without macular sparing, as we expected the incomplete fovea vision would activate participants' coping mechanism of the eyes. In tunnel vision simulation, the center 3° of the visual field were completely visible, which is close to the normal foveal vision. To diminish the effect of the sharp edge of the non-seeing area [40], we empirically set two transparency linear gradients to the degree range of 3°–5° and 5°–10°, respectively.

We updated the location of the non-seeing area (i.e., scotoma) according to the gaze position returned by the eye tracker. Because of the gaze-contingency paradigm, along with the gaze position of participants, the non-seeing area may cover a larger or smaller area of the display. We set the size of the non-seeing area to match the realism of the simulation. For example, in the left hemianopia simulation, when the participants gaze toward the right edge of the screen, the whole screen would be covered, on the contrary, the whole screen would visible when gazing toward the left edge.

E. PROCEDURE

The participants were randomly assigned to six groups (i.e., control group and VFD groups). The control group consisted of 12 students who did not simulate any visual field loss. The remaining participants were evenly assigned to the VFD groups (i.e., each VFD group consist of five participants). However, six participants were selected randomly from the control group for the test-retest repeatability analysis. These participants watched the same additional videos (i.e., two *Tom & Jerry* clips) two times. The gap between the two times was set to one month to lessen the learning effect. To avoid the effect of nuisance factors (e.g., video-watching order), the stimuli were displayed followed a Latin square. The participants were instructed to look at the center area when the buffer image appeared. They were free to move their gaze for the duration of the video and were encouraged to maintain their interest in the videos. One test trial included

[1] SAVAM is available at http://compression.ru/video/savam/ for free using according to Creative Commons 4.0 licenses.

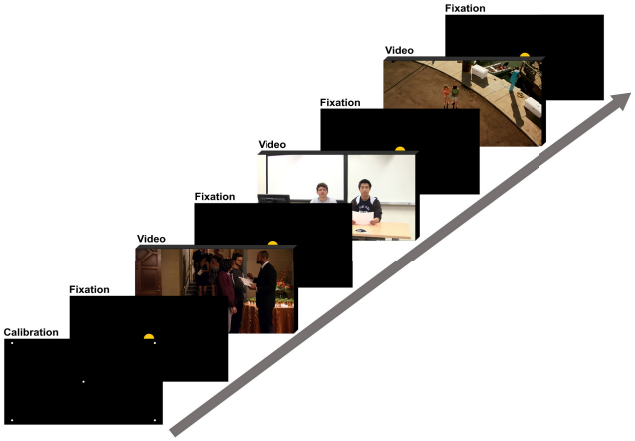

FIGURE 3. Illustration of one session of the test trial–a five-dot calibration was conducted before showing the videos. One test video consists of several SAVAM videos. Each video began with a 3-s buffer image, which was also used to end the session. The duration was controlled within 2 minutes.

two of the same sessions (Figure 3). A 1-min short break was implemented after each session and a 2-min break was encouraged between the two trials. Three practice videos were provided before the real test; because actual patients can gradually adapt to the eye conditions during a long period of visual field evolution [41], the practice session offers participants a transition period to familiarize themselves with the onset of disorders.

The monitor and the chin rest were adjusted to a proper position so the participants felt relaxed and so the center of the buffer image overlapped with their straight gaze. A five-dot tracker calibration provided by Tobii was conducted after every long break. To maintain consistency with subsequent experiments, this step was also performed monocularly. We manually checked whether the tracker needed recalibration according to the proximity between the returned gaze locations and the anchor dots.

We explained the detailed information of this experiment in the consent form. The participants also received an oral briefing (objective, procedures, etc.) just before the test. They were instructed to watch the video according to their own willingness and were asked to relax like they were watching movies at the cinema. The experiment can be finished within an hour if participants clearly understand the briefing and follow the instructions.

F. GAZE PROCESSING

We used an eye tracker to collect the gaze data of the participants when watching videos. The tracker returned 60 raw gaze samples per second, including a timestamp, the horizontal and vertical locations of the gaze in the screen coordinate system, and 3D positions of the gaze and eye origin in the spatial coordinate system.

Following the related study [42], the first step after we obtained the gaze samples was the gap (no-data intervals) fill-in. This process facilitates the filling of data when data are unusually missing due to tracking problems. We filled the gaps via linear interpolation if the gap duration was smaller than the set threshold (75 ms). The samples were then denoised using a median filter (60 ms). Moreover, we used the gaze point as the head and the eye origin as the tail to construct the gaze vector. The Cosines theorem was applied to calculate the angle between each two consecutive gaze vectors. The velocity of one gaze sample was determined by dividing the angle between it and the latter sample by the elapsed time. Movements were classified as fixation if the velocity was $< 1.5\,^\circ/\mathrm{s}$, and we classified a gaze as saccade if the velocity was $> 30\,^\circ/\mathrm{s}$ or the acceleration was $> 8.000\,^\circ/\mathrm{s}^2$ [27]. The movements were defined as smooth pursuit if the velocity was between $1.5\,^\circ/\mathrm{s}$ and $30\,^\circ/\mathrm{s}$ [33]. A fixation group was defined as the combination of a sequence of gaze samples in which all samples were classified as fixation. We describe the location of fixation by the average location within the corresponding group. The timestamp of the fixation is indicated by the first gaze sample of the group, and the duration is defined as the gap between the first and the last gaze sample. We then merged pairwise fixation groups if they were close to each other spatially (0.5°) and temporally (75 ms) [42], [43]. Finally, we discarded the fixation groups whose duration was too short (60 ms) [43] or too long (500 ms) [44].

G. ASSUMPTIONS AND METRICS

In this experiment, we hypothesized that patients with simulated VFDs need to produce more eye movements compared with the control group. In detail, we expect that a specific VFD pattern induces additional eye movements in related directions, i.e., hemianopia leads to more horizontal movements, altitudinal VFD results in more vertical movements, and tunnel vision produces more movements in both directions. This assumption conformed to the previous conclusions about the gaze behaviors of real patients with glaucomatous VFDs when watching the video [33], i.e., more eye movements are required to compensate for the disadvantages.

Based on the assumption, the metric, called eye movement amount (MA) was proposed to describe the characteristics of eye movement. MA was computed as the sum of eye movements toward one direction. Four MA directions were considered, including upward (UMA), downward (DMA), leftward (LMA), and rightward (RMA). To calculate these metrics, we constructed eye movement vectors via two consecutive fixations and decomposed them into horizontal and vertical components. The MA was calculated by adding all the components pointing toward the same direction. The detailed procedures are described as follows:

$$\overrightarrow{mv_i} = P_{i+1} - P_i, \overrightarrow{mv_i} = \overrightarrow{mv_{ix}} + \overrightarrow{mv_{iy}},$$
$$UMA = \sum_{i=1}^{n-1} \left|\overrightarrow{mv_{iy^-}}\right|, DMA = \sum_{i=1}^{n-1} \left|\overrightarrow{mv_{iy^+}}\right|,$$
$$LMA = \sum_{i=1}^{n-1} \left|\overrightarrow{mv_{ix^-}}\right|, RMA = \sum_{i=1}^{n-1} \left|\overrightarrow{mv_{ix^+}}\right|.$$

Here, the eye movement vector $\overrightarrow{mv_i}$ is defined by two fixations, P_i and P_{i+1}. In addition, $\overrightarrow{mv_x}$ and $\overrightarrow{mv_y}$ denote the components of two directions. We define rightward and downward as the positive direction of the X and Y axes as the origin point of the returned gaze data is the left-top corner of the display. Thus x^- and x^+ indicate the leftward and rightward directions, likewise, y^- and y^+ indicate the upward and downward, respectively. Note that in the calculation of MA, we only consider the eye movement of fixation as we empirically assumed that the gaze movement during pursuit would be implicitly included in the distance between the fixation preceding the pursuit episode and the one succeeding it.

H. STATISTICAL ANALYSES

We employed non-parametric statistical tests because of the small sample size. The statistical analysis routine includes a Kruskal-Wallis one-way H test of variance among groups on four aforementioned metrics and all the videos. If a significant difference existed, a post-hoc Mann-Whitney U test with Bonferroni corrections was conducted for pairwise comparisons between the control group and VFD groups. We empirically set the alpha level to 0.05.

Considering the assumption and metrics we proposed, we divided six groups into two sets. The first set (S1) is for analyzing eye movements in the vertical direction, including the control, altitudinal (superior and inferior), and tunnel vision groups. The second set (S2), on the contrary, is for the analyses of eye movements in the horizontal direction. Including the control, hemianopia (left and right), and tunnel vision groups. Two sets underwent the routine independently.

We defined the comparison order of the metrics as UMA → DMA → LMA → RMA. If a significant difference is observed in the pairwise comparison, record it as 1, whereas 0 means no significant difference. If the p-value of the H test is greater than the confidence level, we recorded it as 'X.' The final result was represented by a string of four characters, and each character indicates the analysis result in one specific direction (e.g., in 0-X-1-1, '0' means that for UMA, there is a significant difference among all groups according to the H test but the U test show no significant difference between pairwise groups. 'X' indicates that there is no difference among groups on DMA according to the H test. LMA and RMA both exhibit statistically significant differences and are represented by '1'.)

I. BLAND-ALTMAN METHOD

To evaluate the test-retest repeatability of our experiment, we used Bland-Altman (B&A) plots to determine the agreement between the paired MA values of the two experiments in which we control the same environment (e.g., apparatus, test videos) and participants. The B&A plots quantify the agreement between two measurements by defining the limits of agreement (LoAs) [45]. The upper and lower LoAs are calculated using the mean difference (M) and standard deviation (SD) of the difference (M ± 1.96 SD). The B&A method plots the difference (i.e., Y–axis) between two measurements against the mean (i.e., X–axis) of them. Using this method, 95 % of the data points should fall within the interval of two LoAs [46]. In addition, we expect there is no significant difference between the mean difference of the two measurements with zero (i.e., line of equality), and no proportional bias in the data distribution.

IV. RESULT

A. RESULT OVERVIEW

Table 1 shows the statistical analysis results for our proposed metrics on all the test videos of S1 and S2, respectively. Each column indicates the comparison between a specific VFD pattern and the control, and the result is shown following our aforementioned definition. For S1, most of the result shows no significant difference('X' or '0') in horizontal directions, for S2 on the contrary, most of the result shows no significant difference in vertical directions. This implicitly backs up our assumption of the different distribution of VFDs can lead to different eye movement patterns.

B. AGREEMENT BETWEEN METRICS

Based on our assumptions, i.e., VFD patterns induce additional eye movements toward related directions. We expected with regard to S1 an agreement concerning whether a significant difference exists in LMA and RMA between VFD groups and the control. For S2, we expect an agreement between UMA and DMA similarly. We used Cohen's kappa coefficient to evaluate the agreement between raters (LMA and RMA, as well as UMA and DMA). Note that our calculations of the agreements were based on the existence of a significant difference after the H test, i.e., only considered cases of neither of the two raters were 'X.'

In S1, the H test indicated a significant difference exists in 25 videos. The U test conducted 75 pairwise comparisons between three VFD groups (i.e., tunnel vision, superior, and inferior altitudinal VFDs) with the control group on these videos. Table 2a presents the crosstab of these 75 pairwise comparison outputs of UMA and DMA on S1. In addition, for S2, the H test indicated that there are significant differences in 32 videos. i.e., 96 pairwise comparisons were performed. Table 2b presents the corresponding crosstab of LMA and RMA. The measured Cohen's kappa coefficients were 0.81 (95 % CI: [0.67, 0.96]) for S1 and 0.92 (95 % CI: [0.84, 1.00]) for S2, both of which indicate substantial agreement. These agreements imply the correlations between LMA and RMA, as well as UMA and DMA, which are in line with our assumptions.

C. RESULT OF HEMIANOPIA

For set 2, we mainly explored how VFDs that distribute in the horizontal area of the visual field affect eye movements. We show the number of videos on which participants with artificial hemianopia yielded results consistent with our hypothesis (i.e., produce more eye movement in the horizontal direction) in Table 3. Note that ''Only Left Hemianopia''

TABLE 1. Result overview of statistical analysis on set 1 and set 2.

Videos	Set 1			Set 2		
	Superior	Inferior	Tunnel Vision	Left	Right	Tunnel Vision
v01_Hugo	0-0-0-0	1-1-0-0	0-0-0-0	X-X-1-1	X-X-1-1	X-X-0-0
v02_Dolphin	X-X-X-X	X-X-X-X	X-X-X-X	X-X-X-0	X-X-X-0	X-X-X-0
v03_StepUp	0-0-0-X	1-0-0-X	0-0-0-X	X-X-0-0	X-X-0-1	X-X-0-0
v04_LIVE1	0-0-X-X	0-0-X-X	0-0-X-X	X-X-0-0	X-X-0-0	X-X-0-0
v05_LIVE2	0-0-X-X	1-1-X-X	0-0-X-X	X-X-0-0	X-X-1-0	X-X-0-0
v06_LIVE3	0-0-X-X	0-0-X-X	0-0-X-X	X-X-0-X	X-X-0-X	X-X-0-X
v07_Avatar	0-0-X-0	0-0-X-0	0-0-X-0	X-X-0-0	X-X-0-0	X-X-0-0
v08_Dolphin	X-0-X-X	X-0-X-X	X-0-X-X	X-X-0-0	X-X-0-0	X-X-0-0
v09_StepUpRevolution	X-0-X-X	X-0-X-X	X-0-X-X	X-X-0-0	X-X-0-0	X-X-0-0
v10_VQEG01	0-0-0-X	0-1-0-X	0-0-0-X	X-X-1-1	X-X-1-1	X-X-0-0
v11_VQEG02	X-X-X-X	X-X-X-X	X-X-X-X	X-X-X-X	X-X-X-X	X-X-X-X
v12_VQEG03	X-X-X-X	X-X-X-X	X-X-X-X	X-X-X-X	X-X-X-X	X-X-X-X
v13_IntoTheDeep	X-X-X-X	X-X-X-X	X-X-X-X	X-X-1-1	X-X-1-1	X-X-0-0
v14_Pirates	0-0-X-X	0-1-X-X	0-0-X-X	X-X-0-0	X-X-0-0	X-X-0-0
v15_Sanctum	0-0-X-X	0-1-X-X	0-0-X-X	X-X-1-1	X-X-1-1	X-X-0-0
v16_StepUp	0-0-X-X	1-1-X-X	0-0-X-X	X-X-1-1	X-X-1-1	X-X-0-0
v17_SpiderMan	0-0-0-0	1-1-0-0	1-1-1-1	0-0-1-1	0-0-1-1	1-1-1-1
v18_StepUp	0-0-0-0	1-1-0-0	1-1-1-1	0-0-1-1	0-0-1-1	1-1-1-1
v19_Avatar	X-X-X-X	X-X-X-X	X-X-X-X	X-X-1-1	X-X-1-1	X-X-0-0
v20_DriveAngry	0-0-X-X	1-1-X-X	0-0-X-X	X-X-1-1	X-X-1-1	X-X-0-0
v21_Pirates	0-0-0-0	1-1-0-0	1-1-1-1	0-0-1-1	0-0-1-1	1-1-1-1
v22_VQEG04	X-X-X-X	X-X-X-X	X-X-X-X	0-0-0-0	0-0-1-0	0-0-0-0
v23_VQEG05	X-X-X-X	X-X-X-X	X-X-X-X	X-X-X-X	X-X-X-X	X-X-X-X
v24_VQEG06	X-X-X-X	X-X-X-X	X-X-X-X	X-0-X-X	X-0-X-X	X-0-X-X
v25_Dolphin	X-0-X-X	X-0-X-X	X-0-X-X	X-X-0-0	X-X-1-1	X-X-0-0
v26_Galapagos	X-0-X-X	X-0-X-X	X-0-X-X	X-X-0-X	X-X-0-X	X-X-0-X
v27_UnderworldAwakening	0-0-0-0	1-1-0-0	1-1-1-1	0-0-1-1	0-0-1-1	1-1-1-1
v28_VQEG10	0-X-X-X	0-X-X-X	0-X-X-X	X-X-1-1	X-X-1-1	X-X-0-0
v29_Avatar	0-0-X-X	1-1-X-X	0-0-X-X	X-X-1-1	X-X-1-1	X-X-0-0
v30_Dolphin	0-X-X-X	0-X-X-X	0-X-X-X	X-X-0-0	X-X-0-0	X-X-0-0
v31_DriveAngry	0-0-0-0	1-1-0-0	1-1-1-1	0-0-1-1	0-0-1-1	1-1-1-1
v32_Dolphin	X-X-X-X	X-X-X-X	X-X-X-X	X-X-0-0	X-X-0-0	X-X-0-0
v33_Hugo	0-0-0-1	1-0-0-0	0-0-0-0	X-X-1-1	X-X-1-1	X-X-0-0
v34_VQEG07	0-0-X-X	0-0-X-X	0-0-X-X	X-X-X-X	X-X-X-X	X-X-X-X
v35_VQEG08	X-X-X-X	X-X-X-X	X-X-X-X	X-X-0-0	X-X-0-0	X-X-0-0
v36_VQEG09	0-0-X-X	0-0-X-X	0-0-X-X	X-X-X-0	X-X-X-1	X-X-X-0
v37_UnderworldAwakening	0-0-X-X	1-1-X-X	0-0-X-X	X-X-1-1	X-X-1-1	X-X-0-0
v38_StepUp	0-0-X-X	1-1-X-X	0-0-X-X	X-X-0-0	X-X-1-0	X-X-0-0
v39_Avatar	0-0-X-X	1-0-X-X	0-0-X-X	X-X-1-1	X-X-1-1	X-X-0-0
v42_MSOffice	0-0-0-0	0-0-0-0	1-1-1-1	0-0-1-1	0-0-1-1	1-1-1-1
v43_Panasonic	1-1-X-X	1-1-X-X	0-0-X-X	X-X-1-1	X-X-1-1	X-X-0-0

Each cell indicates the comparison between a specific VFD pattern and the control on corresponding video. Please refer to subsectionIII-H for defination of each notation.

TABLE 2. Crosstab of the Mann-Whitney U test results of two raters on two sets.

Set 1		UMA	
		1	0
DMA	1	20	3
	0	3	49

(a)

Set 2		LMA	
		1	0
RMA	1	45	1
	0	3	47

(b)

TABLE 3. Number of videos in which hemianopia participants produce more horizontal eye movements.

Pattern(s)	Amount of videos (out of 32)
Only Left Hemianopia	0
Only Right Hemianopia	1
Hemianopia	19

(''Only Right Hemianopia'') means only the left (right) hemianopia group has additional horizontal eye movements, whereas the right (left) hemianopia group did not. For the 32 videos (out of 41 videos) that were tested with a significant difference after the H test, the table shows that participants with artificial hemianopia produce additional horizontal eye movements on 19 of them, and either left or right hemianopia will simultaneously induce participants to produce more active eye movement coping mechanisms.

TABLE 4. Number of videos in which altitudinal VFD participants produce more vertical eye movements.

Pattern(s)	Amount of videos (out of 25)
Only Superior VFD	0
Only Inferior VFD	12
Altitudinal VFD	1

D. RESULT OF ALTITUDINAL VFD

For set 1, we expected VFDs that block the vertical parts of the visual field will eventually lead to increased vertical eye movements. Table 4 presents the number of videos on which participants with altitudinal VFD produced a result consistent with our hypothesis (i.e., more vertical eye movements

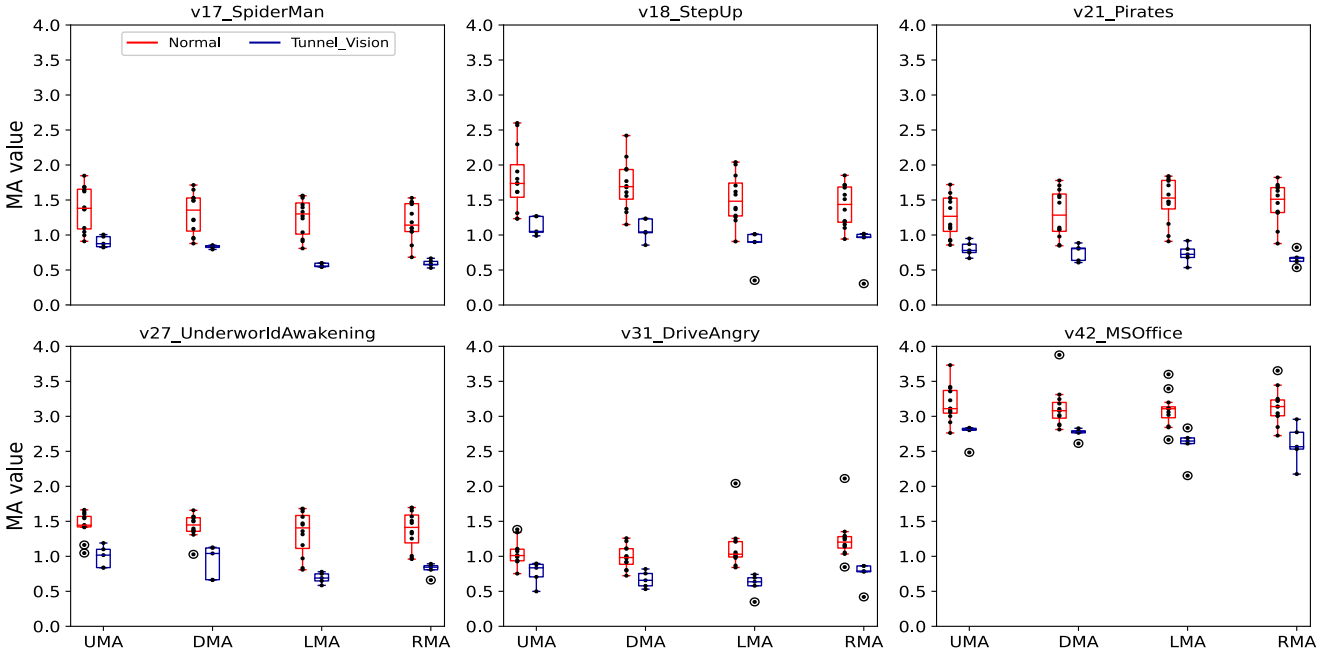

FIGURE 4. MA values of participants in tunnel vision group and control group, in which the tunnel vision group shows statistically significant decreases in eye movements. The x-axis indicates four metrics, and the y-axis indicates the MA values. Blue boxes represent the tunnel vision group, and red boxes indicate the control group. The titles of the subplots represent the video names.

compared to the control). The first two cells indicate the cases of additional eye movements only observed in the corresponding VFD group and not in another one. Active eye movements were observed on 12 videos among participants with inferior VFD. However, for the superior group, on the videos (25/41) that have tested with a significant difference after the H test, most of the pairwise comparisons (24/25) indicate no difference (i.e., no significant difference exists on UMA as well as DMA). We discuss the reasons that superior altitudinal VFDs do not lead to expected eye movements in the next chapter.

E. RESULT OF THE TUNNEL VISION

For the tunnel vision group, we assumed a narrow visual tunnel will activate participants to explore the non-seeing area and eventually lead to increased eye movements amount in all four directions. Table 1 indicates that in both S1 and S2, a significant difference between the tunnel vision group and the control group was observed on six videos. Figure 4 presents a comparison on these videos. Contrary to our assumption, the participants in the tunnel vision group produced significantly decreased MAs in both the horizontal and vertical directions. We observed the results on other videos; as long as the significant difference existed, the corresponding MA value of the tunnel vision participants was smaller, i.e., artificial tunnel vision led to inactive eye movement coping mechanisms in participants. This result is opposite to our assumption but somewhat consistent with previous studies [30], [31] in which decreased saccade amplitude was found in participants with simulated tunnel vision. We discuss the reasons for this in the next chapter.

F. B&A PLOTS

Six participants from the control group attended the experiment twice as mentioned in subsectionIII-E. We controlled the same experiment environment and compared paired MA values between the first time (T1) and the second time (T2) of the experiment. The B&A plots are presented in Figure 5. The distributions of paired MA differences on both videos are consistent with a normal distribution (determined by the Shapiro-Wilk test). In the first clip (Figure 5a), the mean difference in the MA values between T1 and T2 was -0.21 (95 % CI: $[-0.40, 0.82]$), which was not significantly different from zero ($t = 0.68$, $p = 0.50$). This indicates that the experiment yielded comparable MA values at both T1 and T2 on average. The follow-up linear regression analysis indicated there is no proportional bias ($b = -0.17$, $t[22] = -1.52$, $p = 0.14$), which suggests the experiment has a level of agreement. The SD of the difference was 1.51, and the 95 % LoAs was -2.79 to 3.21. In the second clip, a similar conclusion can be drawn (Figure 5b), and the mean difference was -0.36 (95 % CI: $[-1.38, 0.66]$), which was not significantly different from zero ($t = 0.39$, $p = 0.70$). The SD of the difference was 2.55, and the 95 % LoAs was -5.36 to 4.64. The follow-up linear regression indicated no proportional bias ($b = -0.07$, $t[22] = -0.32$, $p = 0.75$).

V. DISCUSSION

This study is an pilot exploration in using a video-watching task and eye-tracking technique to detect VFDs. We assumed that people with VFDs will produce more active eye movements compared to people with normal vision in a video free-watching task. We proposed a new metric that describes

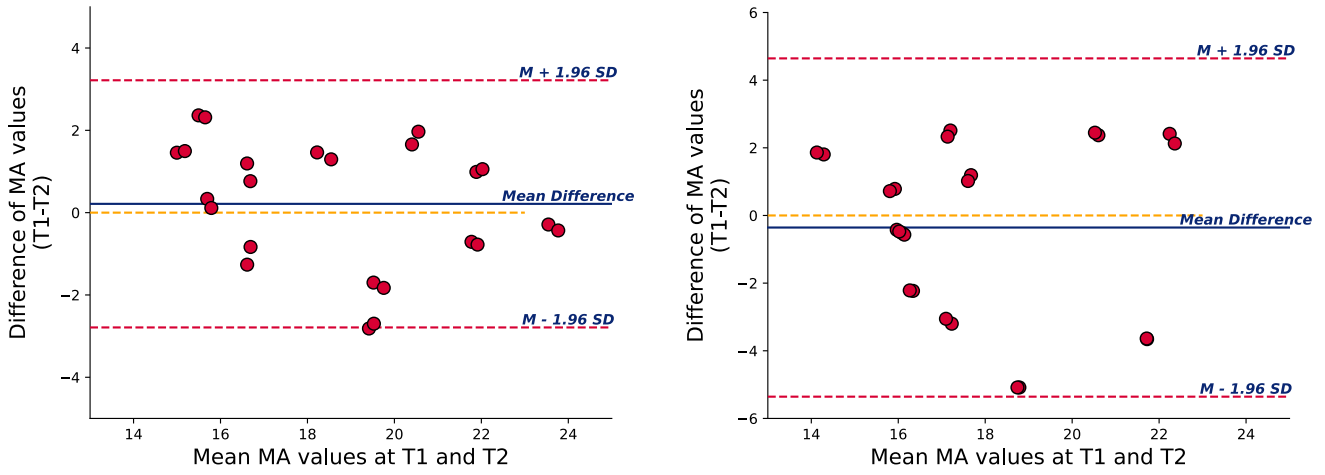

(a) B&A plot on the first video (Flying Cat)

(b) B&A plot on the second video (Tennis Champion)

FIGURE 5. Bland–Altman plots for two measurements with the same participants and experimental environments. The blue solid line represents the mean difference between MA values at time 1 and time 2. The red dashed lines represent the upper and lower 95 % confidence intervals respectively. The yellow dashed line is the reference line of equality.

the eye MA toward a specific direction. Our results indicate that participants with simulated visual field loss have altered eye movement behaviors on specific videos, and the differences are statistically significant. Moreover, the comparison results related to hemianopia as well as inferior VFD were in agreement with our assumptions, i.e., participants belonging to these groups produce more horizontal or vertical eye movements spontaneously. These results indicate that the difference can be potentially used as a biomarker that distinguishes the VFD pattern from the normal pattern.

To confirm our hypothesis in real patient, we recruited a patient with left homonymous inferior quadrantanopia for the experiment. This patient watched the videos in the same controlled environment and the corresponding MA was computed. We used the median value of the control group as the threshold to determine whether this patient produced an increased MA. Because the eye condition of the patient is the part of left hemianopia and inferior altitudinal VFD, we used the result of left hemianopia and inferior VFD as references to the patient's result. The result shows that for the 19 videos on which only participants of the hemianopia groups produced increased horizontal MA, this patient had additional horizontal MA on 16 of them. In addition, for the 13 videos on which only participants of the altitudinal VFD groups have increased vertical MA, the patient had additional vertical MA on 8 of them. Although the patient's pattern is not the same as that in our simulations, the result is still partly consistent with our conclusion, i.e., the difference in MA between patterns can be used as a potential biomarker to distinguish them.

However, tunnel vision participants exhibited decreased MA, which is contrary to our hypothesis and somehow follows the previous findings [30], [31]. To determine the causes of the inactive eye behaviors, we conducted a post survey on participants belonging to the tunnel vision group. The survey question was "how do you feel when you are watching videos with artificial tunnel vision and what makes you not want to move your eyes?" The participants finished the survey individually, after which we collected the responses.

The participants replied that they did not reduce the eye movement activity on purpose. With regard to the feeling of tunnel vision simulation, it can be summarized as follows: (1) there were few clues that the subject did not know what was happening in the non-seeing area in the videos; moreover, the participants only knew what happened within the center area and did not want to lose it; (2) the non-seeing area in the tunnel vision was so overwhelming that the participants did not have any desire to look elsewhere. At least half of the visual field was visible in other VFDs, whereas, in tunnel vision, it can barely be seen. We also believe that the difference in whether the foveal vision is reserved partially causes the different eye movement patterns. Compared with hemianopia or altitudinal VFDs, the simulation of tunnel vision preserved the human's sharpest vision area, whereas, half of the central vision was always blocked in other simulations. This difference may lead to different psychologies of participants during the experiment.

We also attempted to determine why participants with superior VFD did not produce more vertical eye movements, as we had assumed. A post survey was conducted to determine why the participants were reluctant to explore the videos. All the participants replied that they felt tired after watching a few videos and did not want to explore the upper half of the video. The cost of moving the eyes upward was greater than the idea of exploring the video. Two of the participants also mentioned that moving the eye upward was more tiring than toward the other directions. In addition, we believe that the existence of "horizontal bias," when is a tendency of the horizontal saccades are more common than vertical ones [47], also partially affects the participants' eye behaviors. This bias may be caused by the way we carried out the experiment [48], i.e., our test videos were presented

in landscape orientation for more exploration areas in the horizontal direction.

Other experiment limitations that may cause unexpected eye behaviors should be declared. First, we simulated the visual field loss by updating the location of the non-seeing area with the frequency of the tracker's sampling rate (60 Hz). However, the presence of microsaccades [49] may cause jerk-like movements in the non-seeing area. Second, we simulated the non-seeing area with absolute scotoma, whereas the symptoms of VFDs for the real patient may be more complicated. Lower perceptions of contrast, distortions of spatial information, and lower light sensitivity were reported in other studies [50], [51]. Third, the small group size may not provide powerful statistical strength. In addition, it should be noted that the eye behaviors of participants with simulated VFDs may not be completely consistent with the real patient due to their essential difference (i.e., whether they have a VFD).

Future work should focus on the use of metrics to distinguish real VFD patients from normal people and set the threshold of the metric with the highest discrimination ability. In addition, more features should be considered, such as saccade amplitude [34], [52], Bivariate Contour Ellipse Area [53], [54], and new characteristics that can better describe visual behaviors. A comprehensive evaluation can be conducted by analyzing all of the features using machine learning techniques. Furthermore, assessments of the videos are also important. In our result, six videos induce participants of the tunnel vision group to produce an inactive coping mechanism, and these videos have common points. For example, they all have multiple scene changes and multiple objects, and the overall pace of the video is fast (e.g., people running, dancing, or fighting). These features may describe the ability of the videos to be test videos. A suitable test video can naturally guide eye movements and reduce the effect of between-subject variability.

VI. CONCLUSION

In conclusion, by comparing the proposed measurements, the current study explored the different visual behaviors of participants with artificial visual field loss. The results demonstrated that different VFD distributions will cause related eye movement patterns. In addition, the present experiment has a more user-friendly interface and easier requirements as compared with the conventional perimetry. However, how robust these metrics are for application in distinguishing real VFD patients from normal people and what influence this test format can have on the contemporary visual field assessment are still unclear.

REFERENCES

[1] S. L. James, D. Abate, K. H. Abate, S. M. Abay, C. Abbafati, N. Abbasi, H. Abbastabar, F. Abd-Allah, J. Abdela, A. Abdelalim, and I. Abdollahpour, "Global, regional, and national incidence, prevalence, and years lived with disability for 354 diseases and injuries for 195 countries and territories, 1990–2017: A systematic analysis for the global burden of disease study 2017," *Lancet*, vol. 392, no. 10159, pp. 1789–1858, 2018.

[2] P. Nelson, P. Aspinall, O. Papasouliotis, B. Worton, and C. O'Brien, "Quality of life in glaucoma and its relationship with visual function," *J. Glaucoma*, vol. 12, no. 2, pp. 139–150, Apr. 2003.

[3] G. Roberti, G. Manni, I. Riva, G. Holló, L. Quaranta, L. Agnifili, M. Figus, S. Giammaria, D. Rastelli, and F. Oddone, "Detection of central visual field defects in early glaucomatous eyes: Comparison of Humphrey and octopus perimetry," *PLoS ONE*, vol. 12, no. 10, Oct. 2017, Art. no. e0186793.

[4] F. J. Rowe and A. Rowlands, "Comparison of diagnostic accuracy between Octopus 900 and Goldmann kinetic visual fields," *BioMed Res. Int.*, vol. 2014, pp. 1–11, Oct. 2014.

[5] S. Wilscher, B. Wabbels, and B. Lorenz, "Feasibility and outcome of automated kinetic perimetry in children," *Graefe's Arch. Clin. Exp. Ophthalmol.*, vol. 248, no. 10, pp. 1493–1500, Oct. 2010.

[6] B. Bengtsson, J. Olsson, A. Heijl, and H. Rootzén, "A new generation of algorithms for computerized threshold perimetry, SITA," *Acta Ophthalmologica Scandinavica*, vol. 75, no. 4, pp. 368–375, May 2009.

[7] G. Sekhar, "Sensitivity of Swedish interactive threshold algorithm compared with standard full threshold algorithm in Humphrey visual field testing," *Ophthalmology*, vol. 107, no. 7, pp. 1303–1308, Jul. 2000.

[8] S. Shirato, R. Inoue, K. Fukushima, and Y. Suzuki, "Clinical evaluation of SITA: A new family of perimetric testing strategies," *Graefe's Arch. Clin. Exp. Ophthalmol.*, vol. 237, no. 1, pp. 29–34, Jan. 1999.

[9] S. K. Gardiner and S. Demirel, "Assessment of patient opinions of different clinical tests used in the management of glaucoma," *Ophthalmology*, vol. 115, no. 12, pp. 2127–2131, Dec. 2008.

[10] C. Mao, K. Go, Y. Kinoshita, K. Kashiwagi, M. Toyoura, I. Fujishiro, J. Li, and X. Mao, "Different eye movement patterns on simulated visual field defects in a video-watching task," in *Proc. Int. Conf. Cyberworlds (CW)*, Sep. 2020, pp. 153–156.

[11] K. Krafka, A. Khosla, P. Kellnhofer, H. Kannan, S. Bhandarkar, W. Matusik, and A. Torralba, "Eye tracking for everyone," in *Proc. IEEE Conf. Comput. Vis. Pattern Recognit. (CVPR)*, Jun. 2016, pp. 2176–2184.

[12] I. C. Murray, B. W. Fleck, H. M. Brash, M. E. MacRae, L. L. Tan, and R. A. Minns, "Feasibility of saccadic vector optokinetic perimetry: A method of automated static perimetry for children using eye tracking," *Ophthalmology*, vol. 116, no. 10, pp. 2017–2026, Oct. 2009.

[13] I. Murray, A. Perperidis, H. Brash, L. Cameron, A. McTrusty, B. Fleck, and R. Minns, "Saccadic vector optokinetic perimetry (SVOP): A novel technique for automated static perimetry in children using eye tracking," in *Proc. 35th Annu. Int. Conf. IEEE Eng. Med. Biol. Soc. (EMBC)*, Jul. 2013, pp. 3186–3189.

[14] E. Mutlukan and B. E. Damato, "Computerised perimetry with moving and steady fixation in children," *Eye*, vol. 7, no. 4, pp. 554–561, Jul. 1993.

[15] R. Lakowski and P. A. Aspinall, "Static perimetry in young children," *Vis. Res.*, vol. 9, no. 2, pp. 305–312, Feb. 1969.

[16] J. Morales and S. M. Brown, "The feasibility of short automated static perimetry in children," *Ophthalmology*, vol. 108, no. 1, pp. 157–162, 2001.

[17] E. Blumenthal, "The reliability of frequency-doubling perimetry in young children," *Ophthalmology*, vol. 111, no. 3, pp. 435–439, Mar. 2004.

[18] I. C. Murray, L. A. Cameron, A. D. McTrusty, A. Perperidis, H. M. Brash, B. W. Fleck, and R. A. Minns, "Feasibility, accuracy, and repeatability of suprathreshold saccadic vector optokinetic perimetry," *Transl. Vis. Sci. Technol.*, vol. 5, no. 4, p. 15, Aug. 2016.

[19] I. C. Murray, A. Perperidis, L. A. Cameron, A. D. McTrusty, H. M. Brash, A. J. Tatham, P. K. Agarwal, B. W. Fleck, and R. A. Minns, "Comparison of saccadic vector optokinetic perimetry and standard automated perimetry in glaucoma. Part I: Threshold values and repeatability," *Transl. Vis. Sci. Technol.*, vol. 6, no. 5, p. 3, Sep. 2017.

[20] A. D. McTrusty, L. A. Cameron, A. Perperidis, H. M. Brash, A. J. Tatham, P. K. Agarwal, I. C. Murray, B. W. Fleck, and R. A. Minns, "Comparison of threshold saccadic vector optokinetic perimetry (SVOP) and standard automated perimetry (SAP) in glaucoma. Part II: Patterns of visual field loss and acceptability," *Transl. Vis. Sci. Technol.*, vol. 6, no. 5, p. 4, Sep. 2017.

[21] P. R. Jones, N. D. Smith, W. Bi, and D. P. Crabb, "Portable perimetry using eye-tracking on a tablet computer—A feasibility assessment," *Transl. Vis. Sci. Technol.*, vol. 8, no. 1, p. 17, Feb. 2019.

[22] P. R. Jones, D. Lindfield, and D. P. Crabb, "Using an open-source tablet perimeter (eyecatcher) as a rapid triage measure for glaucoma clinic waiting areas," *Brit. J. Ophthalmol.*, vol. 105, no. 5, pp. 681–686, May 2021.

[23] F. W. Cornelissen, K. J. Bruin, and A. C. Kooijman, "The influence of artificial scotomas on eye movements during visual search," *Optometry Vis. Sci.*, vol. 82, no. 1, pp. 27–35, 2005.

[24] J. H. Bertera and K. Rayner, "Eye movements and the span of the effective stimulus in visual search," *Perception Psychophys.*, vol. 62, no. 3, pp. 576–585, Apr. 2000.
[25] N. D. Smith, D. P. Crabb, and D. F. Garway-Heath, "An exploratory study of visual search performance in glaucoma," *Ophthalmic Physiol. Opt.*, vol. 31, no. 3, pp. 225–232, May 2011.
[26] N. D. Smith, F. C. Glen, and D. P. Crabb, "Eye movements during visual search in patients with glaucoma," *BMC Ophthalmol.*, vol. 12, no. 1, pp. 1–11, Dec. 2012.
[27] N. D. Smith, D. P. Crabb, F. C. Glen, R. Burton, and D. F. Garway-Heath, "Eye movements in patients with glaucoma when viewing images of everyday scenes," *Seeing Perceiving*, vol. 25, no. 5, pp. 471–492, Jul. 2012.
[28] D. S. Asfaw, P. R. Jones, V. M. Mönter, N. D. Smith, and D. P. Crabb, "Does glaucoma alter eye movements when viewing images of natural scenes? A between-eye study," *Investigative Ophthalmol. Vis. Sci.*, vol. 59, no. 8, pp. 3189–3198, 2018.
[29] L. Chen, K. Go, Y. Kinoshita, K. Kashiwagi, M. Toyoura, I. Fujishiro, and X. Mao, "Using an eye tracking device to discriminate different symptoms in glaucoma," in *Proc. Int. Conf. Cyberworlds (CW)*, Sep. 2020, pp. 141–144.
[30] A. Cajar, R. Engbert, and J. Laubrock, "Spatial frequency processing in the central and peripheral visual field during scene viewing," *Vis. Res.*, vol. 127, pp. 186–197, Oct. 2016.
[31] A. Cajar, P. Schneeweiß, R. Engbert, and J. Laubrock, "Coupling of attention and saccades when viewing scenes with central and peripheral degradation," *J. Vis.*, vol. 16, no. 2, p. 8, Apr. 2016.
[32] F. Geringswald, E. Porracin, and S. Pollmann, "Impairment of visual memory for objects in natural scenes by simulated central scotomata," *J. Vis.*, vol. 16, no. 2, p. 6, Mar. 2016.
[33] D. P. Crabb, N. D. Smith, F. G. Rauscher, C. M. Chisholm, J. L. Barbur, D. F. Edgar, and D. F. Garway-Heath, "Exploring eye movements in patients with glaucoma when viewing a driving scene," *PLoS ONE*, vol. 5, no. 3, p. e9710, Mar. 2010.
[34] T. C. Kübler, E. Kasneci, W. Rosenstiel, M. Heister, K. Aehling, K. Nagel, U. Schiefer, and E. Papageorgiou, "Driving with glaucoma: Task performance and gaze movements," *Optometry Vis. Sci.*, vol. 92, no. 11, pp. 1037–1046, 2015.
[35] E. J. David, P. Lebranchu, M. P. Da Silva, and P. Le Callet, "Predicting artificial visual field losses: A gaze-based inference study," *J. Vis.*, vol. 19, no. 14, p. 22, Dec. 2019.
[36] D. P. Crabb, N. D. Smith, and H. Zhu, "What's on TV? Detecting age-related neurodegenerative eye disease using eye movement scanpaths," *Frontiers Aging Neurosci.*, vol. 6, p. 312, Nov. 2014.
[37] D. S. Asfaw, P. R. Jones, L. A. Edwards, N. D. Smith, and D. P. Crabb, "Using eye movements to detect visual field loss: A pragmatic assessment using simulated scotoma," *Sci. Rep.*, vol. 10, no. 1, pp. 1–13, Dec. 2020.
[38] B. Gestefeld, A. Grillini, J.-B.-C. Marsman, and F. W. Cornelissen, "Using natural viewing behavior to screen for and reconstruct visual field defects," *J. Vis.*, vol. 20, no. 9, p. 11, Sep. 2020.
[39] V. Lyudvichenko, M. Erofeev, Y. Gitman, and D. Vatolin, "A semiautomatic saliency model and its application to video compression," in *Proc. 13th IEEE Int. Conf. Intell. Comput. Commun. Process. (ICCP)*, Sep. 2017, pp. 403–410.
[40] E. M. Reingold and L. C. Loschky, "Saliency of peripheral targets in gaze-contingent multiresolutional displays," *Behav. Res. Methods, Instrum., Comput.*, vol. 34, no. 4, pp. 491–499, Nov. 2002.
[41] M. C. Leske, A. Heijl, M. Hussein, B. Bengtsson, L. Hyman, and E. Komaroff, "Factors for glaucoma progression and the effect of treatment: The early manifest glaucoma trial," *Arch. Ophthalmol.*, vol. 121, no. 1, pp. 48–56, 2003.
[42] A. Olsen, "The Tobii I-VT fixation filter," *Tobii Technol.*, vol. 21, pp. 1–21, Mar. 2012.
[43] O. V. Komogortsev, D. V. Gobert, S. Jayarathna, D. H. Koh, and S. M. Gowda, "Standardization of automated analyses of oculomotor fixation and saccadic behaviors," *IEEE Trans. Biomed. Eng.*, vol. 57, no. 11, pp. 2635–2645, Nov. 2010.
[44] S. Hoppe, T. Loetscher, S. A. Morey, and A. Bulling, "Eye movements during everyday behavior predict personality traits," *Frontiers Hum. Neurosci.*, vol. 12, p. 105, Apr. 2018.
[45] D. Giavarina, "Understanding bland altman analysis," *Biochemia Medica*, vol. 25, no. 2, pp. 141–151, 2015.
[46] J. M. Bland and D. G. Altman, "Measuring agreement in method comparison studies," *Stat. Methods Med. Res.*, vol. 8, no. 2, pp. 135–160, Jun. 1999.
[47] B. W. Tatler and B. T. Vincent, "The prominence of behavioural biases in eye guidance," *Vis. Cognition*, vol. 17, nos. 6–7, pp. 1029–1054, Aug. 2009.
[48] T. Foulsham, A. Kingstone, and G. Underwood, "Turning the world around: Patterns in saccade direction vary with picture orientation," *Vis. Res.*, vol. 48, no. 17, pp. 1777–1790, Aug. 2008.
[49] S. Martinez-Conde, S. L. Macknik, and D. H. Hubel, "The role of fixational eye movements in visual perception," *Nature Rev. Neurosci.*, vol. 5, no. 3, pp. 229–240, Mar. 2004.
[50] C. X. Hu, C. Zangalli, M. Hsieh, L. Gupta, A. L. Williams, J. Richman, and G. L. Spaeth, "What do patients with glaucoma see? Visual symptoms reported by patients with glaucoma," *Amer. J. Med. Sci.*, vol. 348, no. 5, pp. 403–409, Nov. 2014.
[51] A. S. Hawkins, J. P. Szlyk, Z. Ardickas, K. R. Alexander, and J. T. Wilensky, "Comparison of contrast sensitivity, visual acuity, and Humphrey visual field testing in patients with glaucoma," *J. Glaucoma*, vol. 12, no. 2, pp. 134–138, Apr. 2003.
[52] S. S.-Y. Lee, A. A. Black, and J. M. Wood, "Effect of glaucoma on eye movement patterns and laboratory-based hazard detection ability," *PLoS ONE*, vol. 12, no. 6, Jun. 2017, Art. no. e0178876.
[53] R. B. Goldstein, R. L. Woods, and E. Peli, "Where people look when watching movies: Do all viewers look at the same place?" *Comput. Biol. Med.*, vol. 37, pp. 957–964, Jul. 2007.
[54] E. González, J. Teichman, L. Lillakas, S. Markowitz, and M. Steinbach, "Fixation stability using radial gratings in patients with age-related macular degeneration," *Can. J. Ophthalmol.*, vol. 41, pp. 333–339, Jan. 2006.

CHANGTONG MAO received the B.E. degree in computer science and technology from the Hunan University of Arts and Science, Changde, China. He is currently pursuing the dual M.S. degree in computer science and technology with Hangzhou Dianzi University (HDU), Hangzhou, China, and the University of Yamanashi, Yamanashi, Japan. His research interests include user experience design, human–computer interaction, and machine learning.

KENTARO GO (Member, IEEE) received the B.E. degree in electrical engineering from the University of Yamanashi, Japan, and the M.S. degree in information engineering and the Ph.D. degree in information sciences from Tohoku University. He is currently a Professor with the Department of Computer Science and Engineering, University of Yamanashi. His current research interests include human-centered design, user experience design, human–computer interaction, and telemedicine.

YUICHIRO KINOSHITA (Member, IEEE) received the B.Eng. and Ph.D. degrees in computer science from Ritsumeikan University, in 2002 and 2007, respectively. He is currently an Associate Professor with the Department of Computer Science and Engineering, University of Yamanashi. His current research interests include human–computer interaction, human factors, affective computing, and intelligent systems.

KENJI KASHIWAGI received the M.D. and Ph.D. degrees from Yamanashi Medical University. He is currently a Professor with the Department of Ophthalmology, Faculty of Medicine, University of Yamanashi, Japan. His research interests include the mechanism of glaucoma medicine, the culture of retinal ganglion cells, big-data, and AI application in ophthalmology.

MASAHIRO TOYOURA (Member, IEEE) received the B.Sc. degree in engineering and the M.Sc. and Ph.D. degrees in informatics from Kyoto University, in 2003, 2005, and 2008, respectively. He is currently an Associate Professor with the Department of Computer Science and Engineering, University of Yamanashi, Japan. His research interests include digital fabrication, and computer and human vision.

ISSEI FUJISHIRO (Senior Member, IEEE) received the Doctor of Science in information sciences from The University of Tokyo, in 1988. He is currently a Professor with the Center for Information and Computer Science, Graduate School of Science and Technology, Keio University, Yokohama. His research interests include graphical modeling paradigms, applied visualization design, and smart multi-modal ambient media. He is a Senior Member of ACM and a member of the Science Council of Japan. He has served on the Editorial Board of IEEE TRANSACTIONS ON VISUALIZATION AND COMPUTER GRAPHICS, from 1999 to 2003 and since 2018; *Computers & Graphics* (Elsevier), from 2003 to 2013; and *Visual Informatics* (Elsevier), since 2016. He was a Guest Editor of *IEEE Computer Graphics and Applications* (Vol. 35, No. 6, 2015; Vol. 28, No. 5, 2008). He served as the Chair/the Co-Chair for PacificVAST 2018, CGI 2017, TopoInVis 2017, ACM VRCAI 2015, PacificVis 2014, Cyberworlds 2013, and IEEE SMI 2006; the Program Co-Chair for Cyberworlds 2019, VRCAI 2014, PacificVis 2008, and Volume Graphics 2005/2003; and the SciVis Paper Co-Chair for IEEE VIS 2019 and 2018.

JIANJUN LI received the B.Sc. degree in information engineering from the Xi'an University of Electronic Science and Technology, Xi'an, China, the M.Sc. degree in electrical and computer from The University of Western Ontario, Canada, and the Ph.D. degree in electrical and computer from the University of Windsor, Canada. He is currently the Chair Professor with Hangzhou Dianzi University. His research interests include microelectronics, audio, and video and image processing algorithms and implementation.

XIAOYANG MAO (Member, IEEE) received the B.S. degree in computer science from Fudan University and the M.S. and Ph.D. degrees in computer science from The University of Tokyo. She is currently a Professor with the Department of Computer Science and Engineering, University of Yamanashi, Japan, and an Adjunct Professor with the College of Computer Science, Hangzhou Dianzi University, China. Her current research interests include image processing, visual perception, augmented reality, and their applications to e-health. She received the Computer Graphics International Career Achievement Award, in 2018.